

Supporting Information

Microgel Organocatalysts: Modulation of Reaction Rates at Liquid-Liquid Interfaces

Denise Kleinschmidt ^{a,b,c}, Katja Nothdurft ^d, Mikhail V. Anakhov ^e, Anna Astrid Meyer ^a, Matthias Mork ^a, Rustam A. Gumerov ^{b,e}, Igor I. Potemkin ^{b,e,f,*}, Walter Richtering ^d and Andrij Pich ^{a,b,c,*}

^a Research Area Functional and Interactive Polymers, RWTH Aachen University, Forckenbeckstraße 50, 52062 Aachen, Germany.

^b DWI – Leibniz Institute for Interactive Materials e.V., RWTH Aachen University, Forckenbeckstraße 50, 52062 Aachen, Germany.

^c Aachen Maastricht Institute for Biobased Materials (AMIBM), Maastricht University, Brightlands Chemelot Campus, Urmonderbaan 22, 6167 RD Geleen, The Netherlands.

^d Institute of Physical Chemistry, RWTH Aachen University, Landoltweg 2, 52056 Aachen, Germany.

^e Physics Department, Lomonosov Moscow State University, Leninskie Gory 1-2, Moscow 119991, Russian Federation.

^f National Research South Ural State University, Chelyabinsk, 454080, Russian Federation.

* corresponding authors: pich@dwil.rwth-aachen.de, igor@polly.phys.msu.ru

Synthesis of Microgel-Catalysts Reaction Scheme

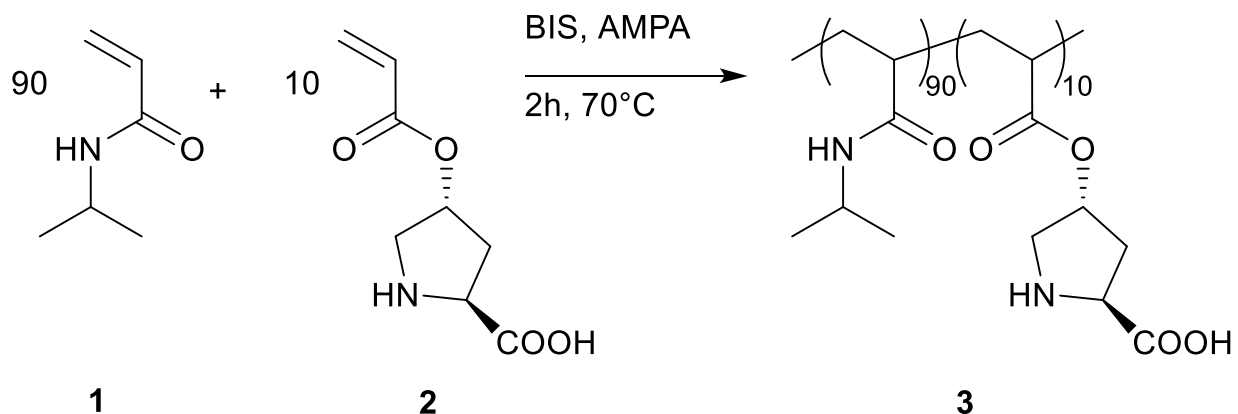


Figure S1. Reaction scheme of free radical precipitation polymerisation in water for synthesis of the microgel-catalysts. The main monomer *N*-isopropylacrylamide (NIPAM, **1**) is polymerised in presence of a polymerisable form of the L-proline organocatalyst (**2**). Synthesis of the latter can be found in literature.^{1,2} As crosslinker for the co-polymer microgel (**3**), the crosslinker *N,N'*-methylenebisacrylamide (BIS) and the initiator 2,2'-azobis(2-methylpropionamidine) dihydrochloride (AMPA) were used.

Characterisation Methods

Thermogravimetric Analysis (TGA)

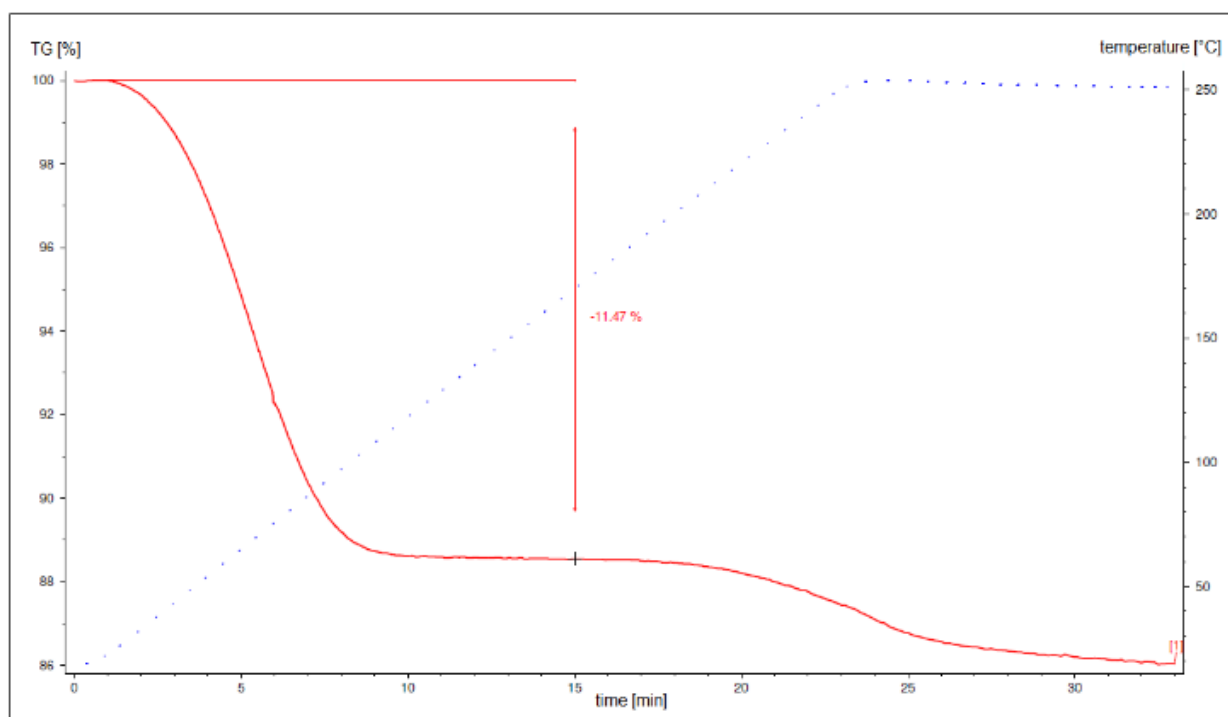


Figure S2. TGA Curve of freeze dried microgel-catalysts used in this work. The red lines represent the mass loss of sample. The blue dotted curve depicts the adapted temperature program.

Attenuated Total Reflection Fourier-transform Infrared Spectroscopy (ATR-FTIR-spectroscopy)

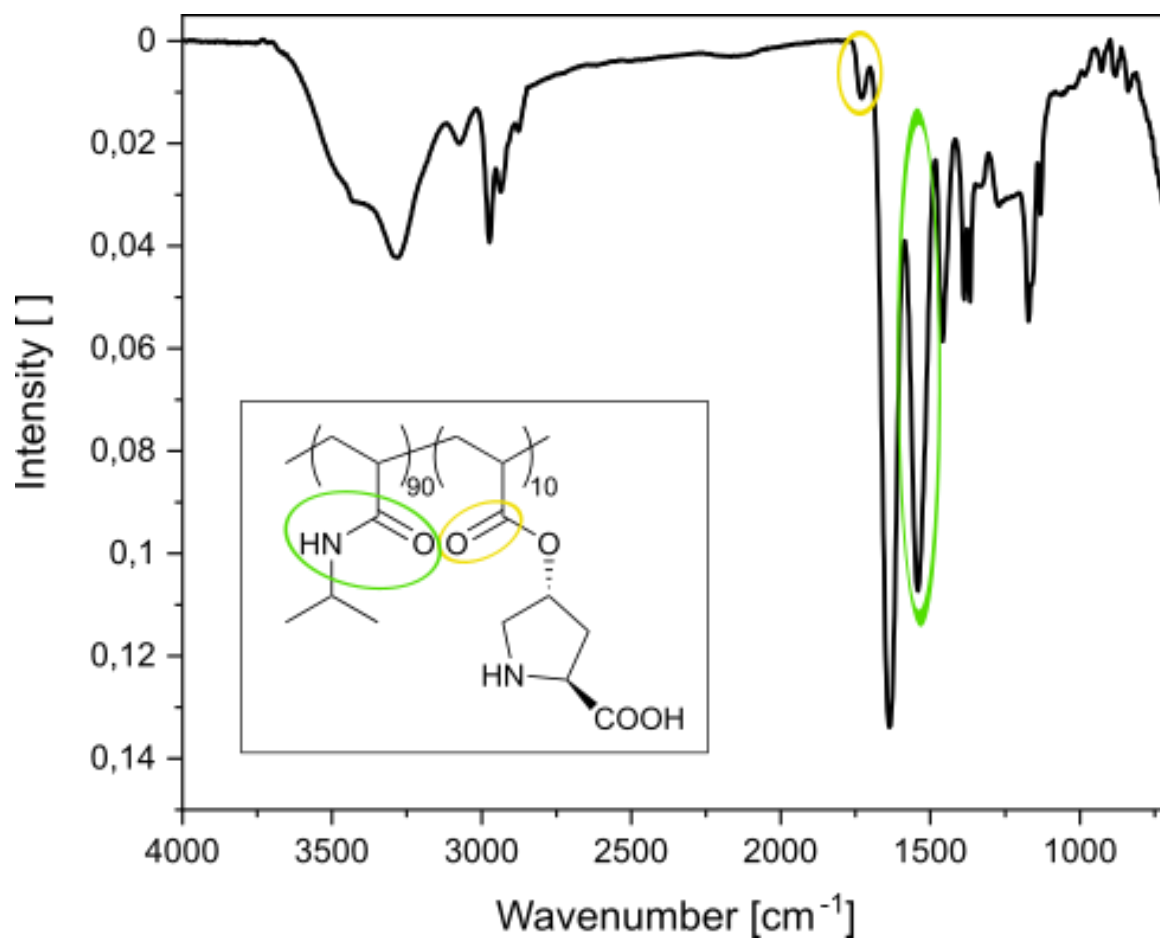


Figure S3. ATR-FTIR spectrum of microgel-catalysts. For calculation of the L-proline content, the intensity ratios of the carbonyl stretching band of the modified L-proline catalysts at 1733 cm⁻¹ ($\nu(\text{C=O})_{\text{L-proline}}$) (yellow) was referenced to the amide II band of NIPAM at 1541 cm⁻¹ ($\nu(\text{amide II})_{\text{PNIPAM}}$) (green). The procedure is in accordance with the literature.^{2,3}

Nuclear Magnetic Resonance Spectroscopy (NMR-spectroscopy)

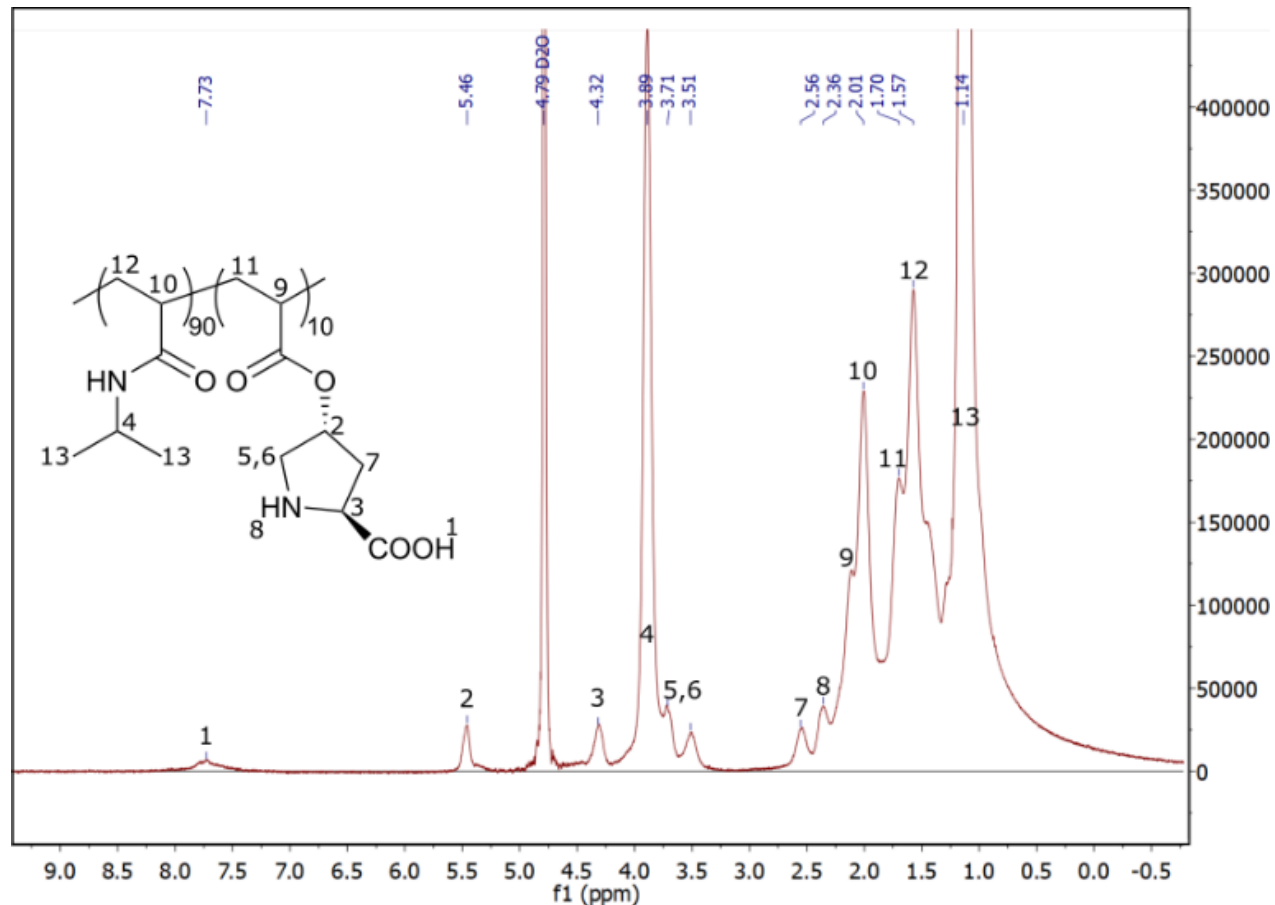


Figure S4. ¹H-NMR spectrum of the microgel-catalysts recorded in D₂O. Due to overlapping of signals, these data were used for qualitative analysis only.

Static Light Scattering (SLS)

SLS measurements were conducted at 25 °C in water, methanol and 20 mol% methanol. In case of water the partly collapsed state at 45 °C and in case of the mixture the partly swollen state at 10 °C were measured additionally. As aggregates were found, especially for the mixture, the 10 °C measurement in the mixture is always performed directly before the 25 °C measurement.

Figure S5a shows the scattering intensity in dependence of the scattering vector q . The microgel-

catalysts are too small to obtain any minima in the q -regime of the SLS. Thus, the scattering curves are analysed with Guinier. The Guinier plots and linear fits of the microgel-catalysts in water (25, 45 °C), methanol (25 °C) and the mixture (10, 25 °C) are shown in **Figure S5b-d**. **Table S1** displays an overview of R_h , R_g and their ratio ρ in water, methanol and 20 mol% methanol at different temperatures.

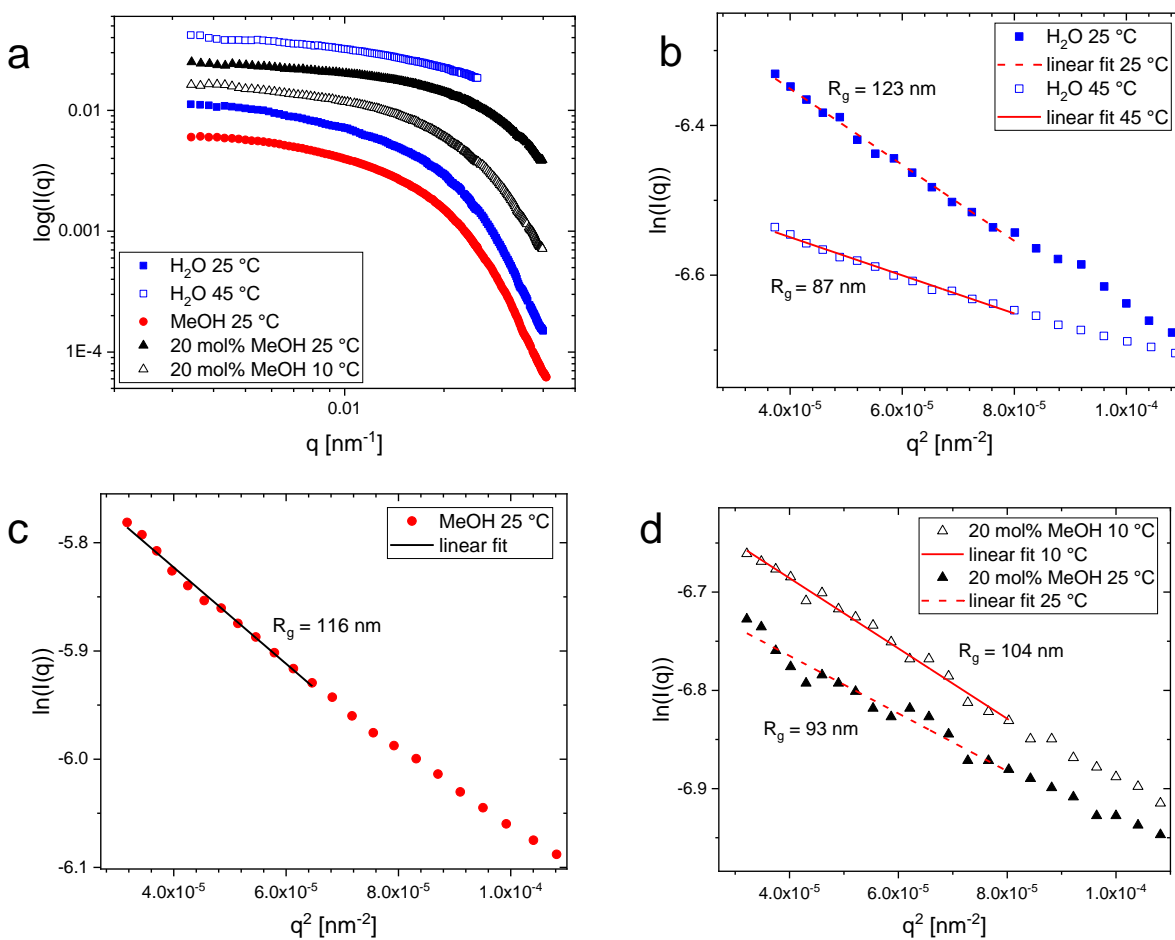


Figure S5. SLS form factors (a) of the microgel-catalysts in various solvents (the curves have been vertically shifted for better visibility) and the corresponding Guinier plots in water (b), methanol (c) and 20 mol% methanol (d).

Table S1. Comparison of the hydrodynamic radius, radius of gyration and their ratio of the microgel-catalysts in different swelling states.

Solvent	T [°C]	R_h [nm]	R_g [nm]	$\rho = R_g/R_h$
Water	25	167 ± 2	123 ± 2	$0,74 \pm 0.012$
	45	110 ± 1	87 ± 2	$0,79 \pm 0.02$
20 mol% MeOH	10	141 ± 1	104 ± 2	$0,73 \pm 0.012$
	25	116 ± 2	93 ± 3	$0,81 \pm 0.03$
MeOH	25	175 ± 7	116 ± 2	$0,66 \pm 0.03$

In general, R_g exhibits comparable trends to R_h concerning the swelling state of the microgel-catalysts: The largest sizes are found in pure water and methanol at room temperature. At 45 °C in water and 25 °C in the 20 mol% mixture the smallest values are found for R_g . Both, R_g and R_h at high temperatures in water are smaller than in the mixture at room temperature. An intermediate value for R_g and R_h is found in the partly swollen state at 10 °C in the mixture. With respect to the ρ -ratio, it is known that a homogeneous sphere exhibits a value of 0.78. Studies by Senff et al.⁴ documented ratios between 0.55 – 0.6 for PNIPAM microgels in the swollen state in water. In comparison, higher ratios close to the one of hard spheres are found in case of the microgel-catalysts. The ρ -ratios lie between 0.66 and 0.81. The smallest ratios are determined for the swollen microgel-catalysts in methanol and water, as well as for the partly swollen state at 10 °C in the 20 mol% methanol mixture. The ρ -ratios close to 0.78 indicate a less fuzzy, more homogeneous structure of the microgel-catalysts compared to pure PNIPAM microgels.

Dissipative Particle Dynamics Simulations (DPD)

Table S2. DPD interaction parameters (in units of $k_B T/r_c$) at $T = 25$ °C used in the simulations. The numbers in brackets in the non-diagonal cells are the corresponding values of Flory-Huggins parameter.

$a_{ij}(\chi_{ij})$	P	L	N	C	W	M
P	25	26.63 ^a (0.50)	30.9 ^a (1.80)	27.16 ^a (0.66)	25.6 ^b (0.18)	25 ^c (0.00)
L	26.63 ^a (0.50)	25	28.37 ^a (1.03)	26.7 ^a (0.52)	25 ^c (0.00)	28,52 ^a (1.07)
N	30.9 ^a (1.80)	28.37 ^a (1.03)	25	29.72 ^a (1.44)	57.73 ^a (10.01)	37.95 ^a (3.96)
C	27.16 ^a (0.66)	26.7 ^a (0.52)	29.72 ^a (1.44)	25	56.35 ^a (9.59)	32.49 ^a (2.29)
W	25.6 ^b (0.18)	25 ^c (0.00)	57.73 ^a (10.01)	56.35 ^a (9.59)	25	^d -
M	25 ^c (0.00)	28,52 ^a (1.07)	37.95 ^a (3.96)	32.49 ^a (2.29)	^d -	25

^a Calculated from Hansen solubility parameter⁵ ^b Calculated using the approach of Yong *et al.*⁶

^c Fixed values ^d The interactions that weren't considered both in experiments and simulations

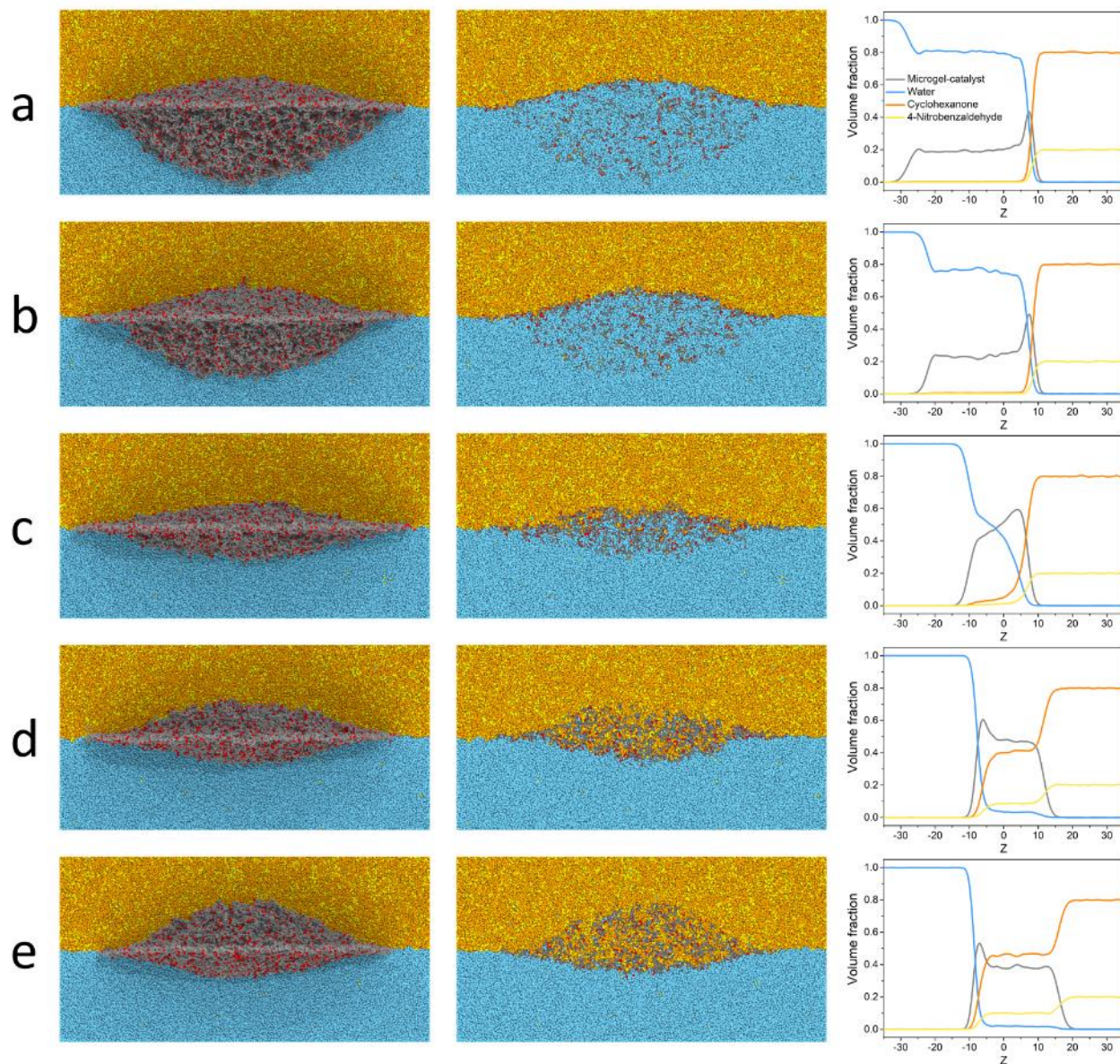


Figure S6. Side views of the adsorbed microgels (left column), cross-section of the microgels through the centre of mass and of PNIPAM (grey), L-proline (red), 4-nitrobenzaldehyde (yellow), cyclohexanone (orange) and water (blue) beads (middle column), concentration profiles along the normal to the interface, z-axis (right column). The lines of different colours correspond to the concentrations of respective types of beads. Different rows correspond to different temperatures: $T = 25\text{ }^{\circ}\text{C}$ (a), $T = 30\text{ }^{\circ}\text{C}$ (b), $T = 35\text{ }^{\circ}\text{C}$ (c), $T = 40\text{ }^{\circ}\text{C}$ (d) and $T = 45\text{ }^{\circ}\text{C}$ (e).

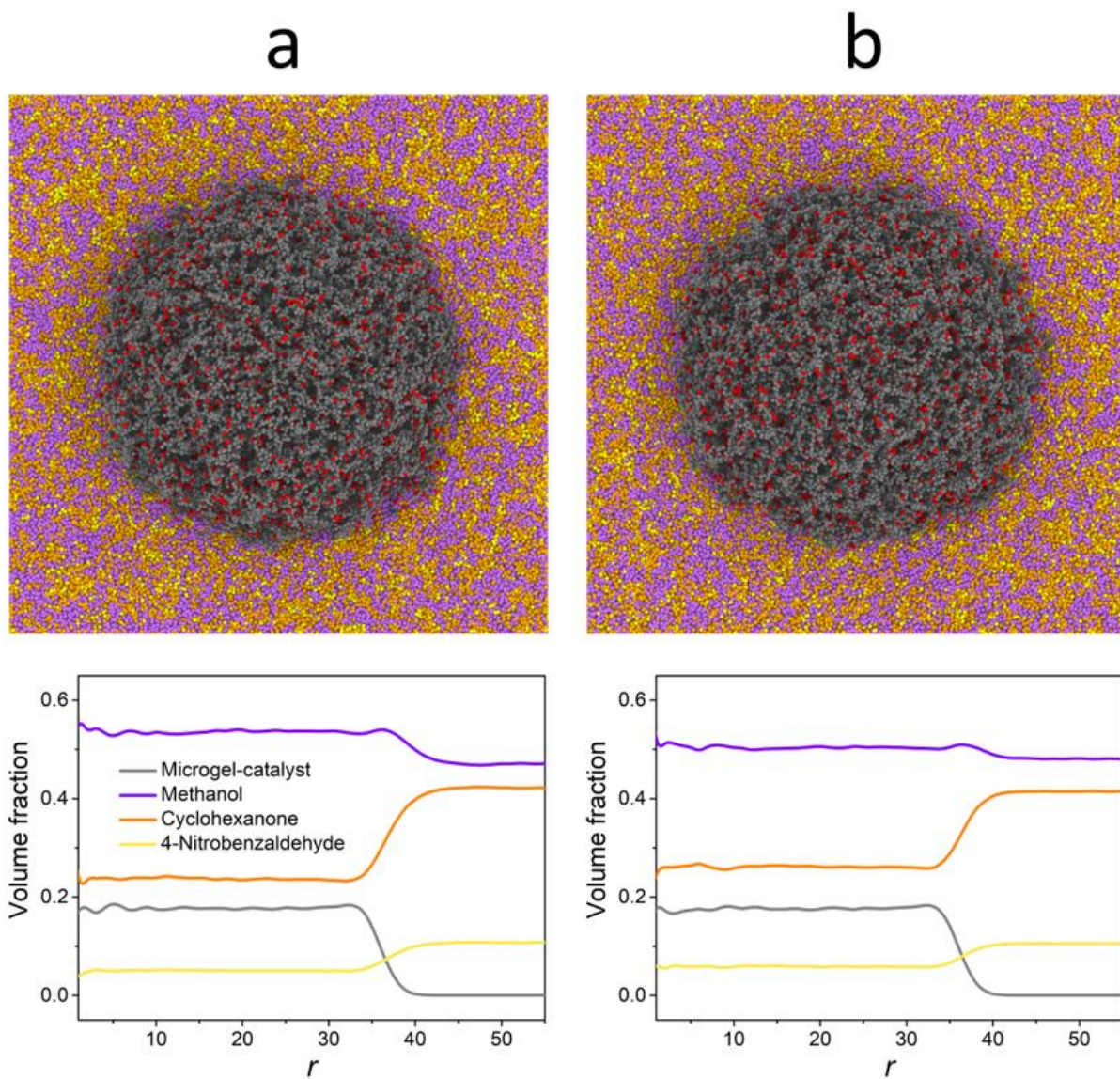


Figure S7. Snapshots of single microgels in methanol-reagents mixture (upper row) and corresponding radial concentration profiles from microgel's centre of mass (lower row) at $T = 25\text{ °C}$ (a) and $T = 45\text{ °C}$ (b). The lines of different colors correspond to the concentrations of respective types of beads: PNIPAM + L-proline (grey), 4-nitrobenzaldehyde (yellow), cyclohexanone (orange) and methanol (purple).

References

- 1 T. E. Kristensen, K. Vestli, K. A. Fredriksen, F. K. Hansen and T. Hansen, *Org. Lett.*, 2009, **11**, 2968–2971.
- 2 D. Kleinschmidt, M. Sofia Fernandes, M. Mork, A. Astrid Meyer, J. Krischel, M. V. Anakhov, R. A. Gumerov, I. I. Potemkin, M. Rueping and A. Pich, *J. Colloid Interface Sci.*, 2019, **559**, 76–87.
- 3 M. E. Jacox, *J. Phys. Chem. Ref. Data*, , DOI:10.1063/1.1497629.
- 4 H. Senff and W. Richtering, *Colloid Polym. Sci.*, 2000, **278**, 830–840.
- 5 C. M. Hansen, *Hansen Solubility Parameters: A User's Handbook*, CRC Press, Boca Raton, 2nd edn., 2007.
- 6 X. Yong, O. Kuksenok, K. Matyjaszewski and A. C. Balazs, *Nano Lett.*, 2013, **13**, 6269–6274.